Fabrication of an Array of Eccentric Sources for Freehand Optical Ultrasound Imaging

Fraser T. Watt*,†, Sacha Noimark*,†, Adrien E Desjardins*,†, Paul C. Beard*,†, Erwin J. Alles*,†,
*Wellcome / EPSRC Centre for Interventional and Surgical Sciences, University College London, London, UK
†Department of Medical Physics & Biomedical Engineering, University College London, London, UK

***Abstract*—Free-hand optical ultrasound (OpUS) imaging is an emerging ultrasound imaging paradigm that utilises an array of fiber-optic sources and a fiber-optic detector to achieve video-rate, real-time imaging, with a flexible probe. Previous designs used multimode fibers to achieve circular OpUS sources that emitted divergent fields propagating away from the imaging plane, resulting in image artefacts and reduced penetration depths. The directivity of the emitted ultrasound field can be optimised by changing the trasnducer shape, moving to eccentric transducers can improve elevational confinement and associated aretefacts. In this work, methods for fabricating suitably eccentric waveguides that can be placed distally to a fiber-bundle array probe are presented. In addition, the scalability of one of these methods is demonstrated by fabricating a ten-element array of waveguides.**

***Index Terms*—Optical Ultrasound, Waveguides, Source Directivity, Rapid Prototyping**

I. Introduction

Optical Ultrasound (OpUS) imaging is an ultrasound imaging modality in which ultrasound is both transmitted and detected through optical means. Ultrasound is generated by the selective application of the photoacoustic affect, when excitation light is incident upon an absorbing material that is typically deposited at the tip of a optical fiber or formed into a membrane [1]–[3]. The detection elements of an OpUS imaging device are typically fiber-based and utilise optically resonant detectors, such as Fabry-Pérot cavities [4], [5] or ring resonators [6]. In some cases direct interferometry [7], [8] is used in non-contact studies.

OpUS imaging has been performed successfully with two-fiber probes, comprising seperate detector and transmitter fibers, mounted together. Such two-fiber probes can be either front [9] or side viewing [10]. Whilst these miniature probes are effective and can achieve impressive imaging quality, they require some form of mechanical translation, such as rotation around a central axis or lateral motion, to form an imaging aperture which typically results in long imaging times. An alternative paradigm has been implemented in bench-top OpUS imaging systems, which use galvanometric mirrors to generate an array of ultrasound sources on a monolithic membrane, with a detector placed either close to the membrane or at a distance. These devices can achieve high frame rates and excellent imaging quality; however, these systems are not designed for use outside of the laboratory environment in their current form.

Free-hand OpUS imaging probes are an emerging paradigm that combine the strengths of two-fiber and bench top probes. Free-hand probes are constructed from an array of fiber optic OpUS sources, with a single fiber-optic detector, that are capable of performing real-time, video-rate, synthetic aperture ultrasound imaging, in a compact and flexible form factor that resembles that of current piezoelectric technologies [11]. Existing probes have achieved a high frame rate, however the image contrast was limtited by specific aspects of the probe design. This probe used optical fibers to transmit light into an OpUS generating material, resulting in small, circular, ultrasound sources. As a result, the emitted ultrasound fields were isotropic and highly divergent, and a significant portion of the ultrasound power was hence radiated away from the imaging plane. This results in significant out-of-plane artefacts and reduced in plane pressures, particularly for high-bandwidth OpUS devices. Selective bandwidth filtering may suppress artefacts arising from higher frequency components, at the expense of the corresponding spectral power, further limiting the SNR of the device.

Confinement of ultrasound waves to the imaging plane can be improved by using eccentric as opposed to circular sources [12], [13]. In free space this can be achieved through the use of a cylindrical lens or by tilting an array of circular optical fibers [14] relative to the generating surface. However, in a free-hand probe these methods are not viable, cylindrical lenses would require extremely short working distances to generate effective OpUS sources, and both options would require free-space optical paths that require bulky probe designs, high-quality optics with extremely short focal lengths, or air-filled cavities, which are impractical for a contact-based probe.

In this work we present four methods for generating a suitably eccentric OpUS source by shaping the light output from an array of circular optic fibers. Two approaches are presented here: holographic manipulation of the illumination profile through the use of eccentric light shaping diffuser sheets, and the fabrication and application of eccentrically shaped waveguide sections. Each method was then coupled with a carbon-nanotube loaded PDMS (CNT-PDMS) film to form an OpUS source, and characterised acoustically. Finally, a ten-element array of 3D-printed optical waveguides is presented, demonstrating the suitability and scalability of one of

This work was supported by the Wellcome Trust (203145Z/16/Z), the Engineering and Physical Sciences Research Council (EPSRC) (NS/A000050/1, EP/N021177/1, EP/S001506/1,EP/N509577/1,EP/T517793/1), and the Rosetrees Trust (PGS19-2/10006).

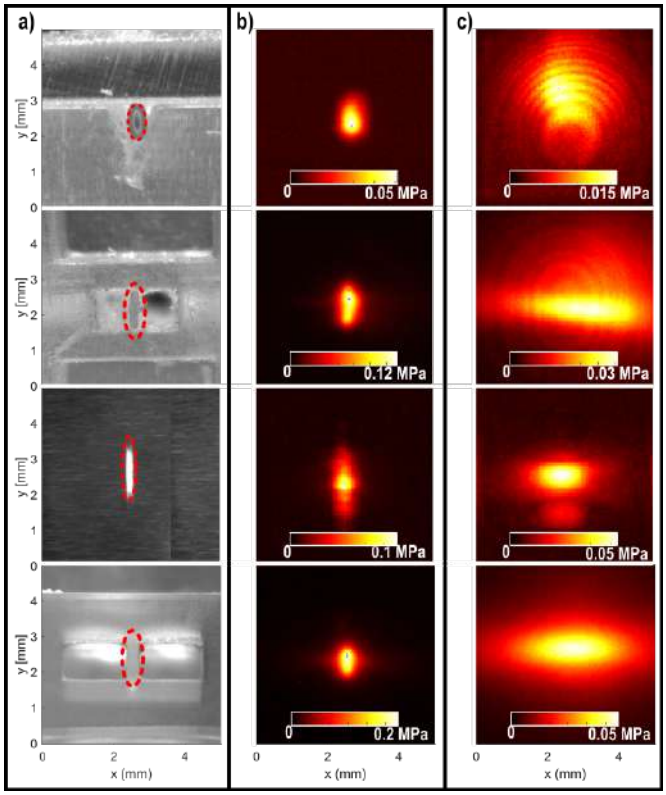

Fig. 1. **Images and ultrasound field scans of single-element eccentric OpUS source generation methods. Top-to-bottom:** Compressed polymer optic fiber, 0.1 mm by 1 mm eccentric capillary waveguide, 60:1 light shaping diffuser film, 0.2 mm by 1 mm 3D printed waveguide. **a)** Magnified image of active components, with active areas outlined. **b)** 1.5 mm acoustic field scan of individual sources. **c)** Acoustic field propagated to 10 mm from source by the angular spectrum approach.

the demonstrated methods to generate an array of eccentric OpUS sources for a handheld probe.

II. Methods

To shape the output from a circular fiber two methods were considered: transmission of light through a light shaping diffuser (LSD) film and transmission through a suitably shaped waveguide.

A. Eccentric Light Shaping Diffuser

The first method considered was the application of a holographic light-shaping diffuser (LSD) film to shape the excitation light without the use of waveguides. An anisotropic diffuser with 60°by 1°divergence angle (L60X1E5-12 HIGH TECH, Luminit, Torrance, Canada) was placed at the distal end of an optical fibre (105 µm, Thorlabs, FG105LCA), and the emitted divergent light propagated through a 3 mm thick acrylic layer to yield an illumination spot of ca. 1 mm by 150 µm.

B. Eccentric Waveguides

Three methods were used to fabricate eccentric optical waveguides: reshaping polymer optic fiber (POF) sections, filling rectangular glass capillaries with an epoxy with a higher refractive index than glass, and direct 3D printing of rectangular waveguide structures.

The first method attempted was to reshape polymer optic fiber (POF). POF is regularly reshaped by controlled heating and compression to improve packing in commercial fiber bundles or create optical couplers [15]. Short sections (ca. 5 cm) of 200 µm diameter core, 500 µm diameter polymer optic fiber (MedPOF/200-PC-SM, Chromis Fiberoptics) were fixed between two pieces of acrylic and pressure was applied by tightening screws. This assembly was then immersed in a heated water bath (IKA HBR 4 Control) at 95°C for 15 minutes. Subsequently, the screws were then tightened further, before a additional 15 minutes heating. The assembly was removed and allowed to cool, before the fiber was removed. This yielded a tapered waveguide, which was manually cleaved using a scalpel in the compressed section. The resulting end face had dimensions of 0.558 ± 0.05 mm (long axis) by 0.135 ± 0.02 mm (short axis).

Second, glass capillaries have been used as an optical waveguide, either without modification where light is coupled into the glass wall to form a ring waveguide [16] or by filling the lumen with a high-index medium to act as a waveguide core [17]. To fabricate eccentric waveguides, capillaries (lumen: 1 mm by 0.1 mm, VitroTubes 5010, Vitrocom) were laser cut to 2 cm lengths, and filled with a high-index UV curable adhesive (NOA81, Norland Products, published refractive index: 1.56) via capillary action and cured with a UV LED (M365FP1, Thorlabs). To remove any excess glass and provide a flat surface for optimal optical coupling, the filled capillary waveguides were fixed in a custom 3D printed frame and manually polished.

Third,direct 3D printing of optical waveguides was investigated as readily scalable and versatile alternative to filled capillaries or shaped POF. A commercial grade stereolithography (SLA) printer (Form 3, Formlabs) was used to print two test pieces of optically clear resin (RS-F2-GPCL-04 Clear Resin V4, Formlabs) at a 25 µm layer height, which was then washed in isopropyl alcohol and cured at manufacturer recommended specifications. These test pieces were then analysed using differential absorbtion spectroscopy and shown to have low absorption in the visible spectrum (0.8% at 532 nm) and around 1064 nm (approximately 0.1%), however in other areas of the near-infrared (NIR) absorption of up to 60% was found. The same printer and resin were then used to print rectangular waveguides of dimensions 0.2 mm (width) by 1mm (height) by 20 mm (length), similar to the filled glass capillary waveguides tested previously. The waveguides were printed on a supporting frame comprising fourteen orthogonal struts (400 µm in thickness) to prevent warping. The waveguide was then coated in a low-index UV cured adhesive (NOA85, Norland Products, published refractive index: 1.46) which acts as cladding; the end faces of the waveguide were manually polished.

Each of the eccentric waveguides was butt-coupled to a multimode optical fiber (105 µm, Thorlabs, FG105LCA) and

illuminated with light of wavelength 1064 nm, and tested for power transmission. Compressed POF achieved a maximum transmission of 90%, filled capillary waveguides were capable of up to 83% transmission, and direct printed waveguides were capable of up to 85% transmission, demonstrating limited leakage into the surrounding frame structure.

C. Acoustic Characterisation

To assess the OpUS generation performance of all four options considered, each of the four illumination assemblies was covered by a CNT-PDMS membrane. Excitation light (wavelength: 1064 nm; pulse duration: 2 ns; pulse energy: 2.8 µJ; repetion rate: 1 kHz; DSS1064-Q4, Crylas, Germany) was delivered via a butt-coupled fibre (105 um; Thorlabs, FG105LCA). To facilitate alignment and handling, the three waveguides were embedded into custom 3D printed holders. The generated OpUS field was then measured at approximately 1.5 mm from the waveguide surface by scanning a calibrated 200 µm needle hydrophone (Precision Acoustics) across a 5 mm by 5 mm area, at 50 µm step size. The resulting pressure traces were bandpass filtered at 2 to 25 MHz and envelope detected through a Hilbert transform. To characterise the propagation of the ultrasound field from each source, the planar field scans were numerically propagated using the angular spectrum approach [18].

D. 10-Element 3D Printed Array Fabrication and Characterisation

To assess the scalability of 3D printing waveguides to a full array, a 10-element waveguide array was designed and fabricated. To facilitate accurate and dense element packing, the array was printed as two 5-element arrays at 800 µm element pitch, and then interleaved to form a 10-element array at 400 µm pitch. The two array halves were fixed with low-index UV-cured adhesive (acting as waveguide cladding) and polished manually. Each of the waveguides was butt-coupled to one of ten separate fibres (105 µm; Thorlabs, FG105LCA), which were aligned using a custom laser cut acrylic substrate. A CNT-PDMS membrane was fixed to the front of the waveguide array to act as an OpUS generator. A galvanometric mirror scanning system (mirrors: GVSM002, Thorlabs, Germany; lens: 50 mm focal length; LBF254-050-C, Thorlabs, Germany) was used to couple focussed, pulsed excitation light into the fibers sequentially (1064 nm wavelength; 1.5 ns pulse duration; 1 kHz pulse repetition rate; DSS1064-Q4, Crylas Germany). An acoustic field scan for each source was performed with a calibrated needle hydrophone over a 10 mm (lateral) by 4 mm (elevational) area at 50 µm step size. The resulting pressure traces were bandpass filtered at 2 to 25 MHz and envelope detected through a Hilbert transform.

III. Results

When illuminated with white light it was confirmed that each each of the four methods considered resulted in the generation of an elliptical light spot. This resulted in the generation of highly eccentric OpUS pressure fields (Fig. 1), with the wide

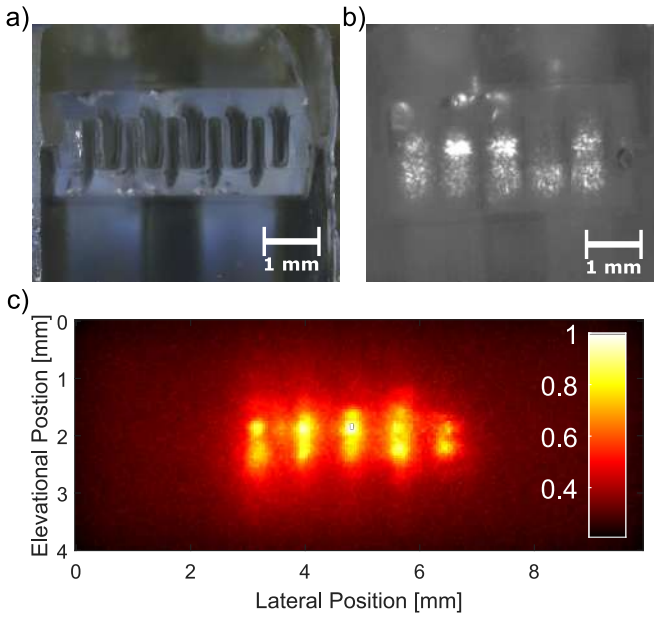

Fig. 2. **Demonstration of a 10-element 3D printed waveguide array a)** Magnified image of fabricated and polished 10-element eaveguide array. **b)** Magnified image of waveguide face with alternating sources illuminated. **c)** Normalised, composite ultrasound field scans of alternating OpUS sources in 10 element 3D printed waveguide array.

Method	Maximum Pressure (MPa)	Peak Frequency (MHz)	-6 dB Bandwidth (MHz)
LSD	0.106	9.28	28.8
Compressed POF	0.048	8.54	28.7
Capillary Waveguide	0.121	13.06	26.2
3D printed Waveguide	0.222	12.82	30.9
Printed waveguide Array	0.055 ± 0.03	13.7 ± 0.8	26 ± 2

TABLE I
MAXIMUM PRESSURE, PEAK FREQUENCY AND BANDWIDTH FOR EACH OF THE METHODS PRESENTED.

badwidth typical for OpUS sources. Compressed POF yielded the lowest peak pressures (table I), likely due to issues with optical coupling between the 105 µm fiber and the POF, the capillary waveguide and LSD generated eccentric spots with similar pressure and spot shapes, with the capillary waveguide generating a more even pressure distribution. The most promising method was through the 3D printed waveguide, which generated pressures in line with those seen with a circular fiber source, despite the larger surface area. Numerically propagated field scans revealed that the POF and LSD propagations demonstrate non-uniform shapes. In the case of the POF this was likely a result of low measured pressures arising from poor optical coupling ionto the waveguide and an uneven end face of the waveguide. The LSD propagation suggests that there may be optical grating lobes causing additional ultrasound hot spots in the field shape, which could deteriorate image quality. Both the 3D printed and capillary waveguides demonstrate effective confinement to the imaging plane across the propagation; however, only the 3D printed waveguide generated a symmetric shape with even pressure distribution.

Ultrasound characterisation of the 10-element 3D printed array demonstrated that each of the ten sources could be excited individually without cross-talk. All sources in the array demonstrated eccentric sources, of approximately equal dimensions.

IV. Discussion and Conclusion

In this work four different methods were preneted that all yielded eccentric illumination and OpUS source geometries, in a manner that could be incorporated into a hand-held OpUS imaging probe. Eccentric sources have the capacity to significantly improve the imaging quality of OpUS imaging devices, and the ability to generate eccentric sources from the output of a cost-effective circular fiber in a compact manner may lead to improved imaging with both the hand-held array probes considered here as well as two-fiber devices.

Whilst all methods outlined in this paper generated eccentric OpUS sources, not all are scalable to an array of arbitrary geometry. Compressed POF generated low ultrasound pressures and less elliptical field shapes, along side this the compression of the fiber was not reproducible across multiple samples, however this may be effective for smaller, two fiber probes that only require a single elliptical source. Similarly, whilst effective in a single waveguide, the range of geometries commercially available limits the effectiveness of capillary waveguides. In addition, the actual shape and size of the lumen of capillaries may vary significantly between different batches, which would complicate the accurate fabrication of arrays containing large numbers of waveguides. The LSD design was effective and more compact than the other methods presented here, and would enable a more compact probe, however the presence of optical grating lobes in the LSD propagation may lead to additional artefacts when used in a full imaging probe. In addition, the required acrylic stand off and sealing result in transducer sizes that extend significantly beyond the illumination geometry.

The most effective method presented in this paper is direct SLA printing of optical waveguides, with both effective shape control and the most well-behaved OpUS generation of the four methods discussed here. The versatility of 3D printing would enable a range of potential OpUS shapes, as well as the possibility of a range of probe geometries, including tightly curved waveguides. The optical and OpUS performance of the 3D printed waveguides presented here confirm that 3D printing of optical components operating in the near-infrared is feasible, at least for a wavelength of 1064 nm. It has also been demonstrated that an array of waveguides can be printed in an effective manner and be used to generate an array of approximately equal OpUS sources. Some of the ten elements in the waveguide array emitted pressure fields exhibiting lower pressure amplitudes or asymmetry; this is likely caused by damage sustained during assembly. For future arrays, the assembly process will be simplified to avoid damage, and performance variation can be compensated in post-processing. While here an array comprising just ten elements is presented, the fabrication process is readily scaled up to arrays comprising dozens of elements. Printed optical waveguides present an extremely versatile and adaptable method of shaping optical field shapes over short distances. This method can be applied to visible wavelength, and has been demonstrated to be effective for 1064 nm, one of the most commonly used wavelegnths in a range of fields; however, the high absorbtion in other areas of the NIR may restrict use in certain applications.

References

[1] Paul Beard. Biomedical photoacoustic imaging. *Interface focus*, 1:602–631, 2011.

[2] Sacha Noimark, Richard J. Colchester, Radhika K. Poduval, et al. Polydimethylsiloxane composites for optical ultrasound generation and multimodality imaging. *Advanced Functional Materials*, 28:1–16, 2018.

[3] Sung Liang Chen. Review of laser-generated ultrasound transmitters and their applications to all-optical ultrasound transducers and imaging. *Applied Sciences (Switzerland)*, 7, 2017.

[4] B T Cox, E Z Zhang, J G Laufer, and P C Beard. Fabry perot polymer film fibre-optic hydrophones and arrays for ultrasound field characterisation. *Journal of Physics: Conference Series*, 1:32–37, 2004.

[5] James A. Guggenheim, Jing Li, Thomas J. Allen, et al. Ultrasensitive plano-concave optical microresonators for ultrasound sensing. *Nature Photonics*, 11:714–719, 2017.

[6] Wouter J. Westerveld, Md Mahmud-Ul-Hasan, Rami Shnaiderman, et al. Sensitive, small, broadband and scalable optomechanical ultrasound sensor in silicon photonics. *Nature Photonics*, 15:341–345, 2021.

[7] Jami L. Johnson, Mervyn Merrilees, Jeffrey Shragge, and Kasper van Wijk. All-optical extravascular laser-ultrasound and photoacoustic imaging of calcified atherosclerotic plaque in excised carotid artery. *Photoacoustics*, 9:62–72, 2018.

[8] Xiang Zhang, Jonathan R. Fincke, Charles M. Wynn, Matt R. Johnson, Robert W. Haupt, and Brian W. Anthony. Full noncontact laser ultrasound: first human data. *Light: Science and Applications*, 8, 2019.

[9] Erwin J. Alles, Sacha Noimark, Edward Zhang, Paul C. Beard, and Adrien E. Desjardins. Pencil beam all-optical ultrasound imaging. *Biomedical Optics Express*, 7:3696, 2016.

[10] Richard J. Colchester, Callum Little, George Dwyer, et al. All-optical rotational ultrasound imaging. *Scientific Reports*, 9:1–8, 2019.

[11] Erwin J Alles, Eleanor C Mackle, Sacha Noimark, Edward Z Zhang, Paul C Beard, and Adrien E Desjardins. Freehand and video-rate all-optical ultrasound imaging. *Ultrasonics*, 116:106514, 2021.

[12] Erwin J Alles, Sacha Noimark, Efthymios Maneas, et al. Video-rate all-optical ultrasound imaging. *Biomedical optics express*, 9:3481–3494, 2018.

[13] Erwin J. Alles and Adrien E. Desjardins. Source density apodization: Image artifact suppression through source pitch nonuniformity. *IEEE Transactions on Ultrasonics, Ferroelectrics, and Frequency Control*, 67:497–504, 2020.

[14] David Thompson, Hindrik Kruit, Damien Gasteau, and Srirang Manohar. Laser-induced synthetic aperture ultrasound imaging laser-induced synthetic aperture ultrasound imaging. *Journal of Applied Physics*, 163105, 2020.

[15] Kwang Taek Kim, Byeong Ha Lee, Cherl-Hee Lee, and Jonghun Lee. Fabrication and characterization of n×n plastic optical fiber star coupler based on fused combining. *Korean Journal of Optics and Photonics*, 24:17–22, 2013.

[16] Nicolino Stasio, Atsushi Shibukawa, Ioannis N. Papadopoulos, et al. Towards new applications using capillary waveguides. *Biomedical Optics Express*, 6:4619, 2015.

[17] RIchard J. Colchester, C Allum D. Little, Erwin J. Alles, and Adrien E. Desjardins. Flexible and directional fibre optic ultrasound transmitters using photostable dyes. *OSA Continuum*, 4:2488–2495, 2021.

[18] Xiaozheng Zeng and Robert J. McGough. Optimal simulations of ultrasonic fields produced by large thermal therapy arrays using the angular spectrum approach. *The Journal of the Acoustical Society of America*, 125:2967, 2009.